Multidisciplinary Study of Pulse Detonation Engines
Principal Investigator: J.E. Shepherd

Graduate Aeronautical Laboratories,
California Institute of Technology
Pasadena, California 91125

Research at the Explosion Dynamics Laboratories at Caltech over the past three years under an ONR contract has examined many issues critical to Pulse Detonation Engine (PDE) development. These include: fundamental and applied studies of detonation initiation; detonation cell width measurements to characterize fuels, including JP10; visualization of the reaction zone structure of propagating detonations; direct measurements and analytical modeling of impulse from a detonation tube, including the effects of partial fill and exit geometry; studies of detonation diffraction; and the structural response of tubes to detonation loading, including fracture and failure. Each of these aspects of our program is discussed and key results are presented.

Detonation Initiation

A variety of techniques for detonation initiation in insensitive fuel-air mixtures (such as JP10 and air, or propane and air) for air-breathing PDE applications were investigated, including transition from flame to detonation, hot turbulent jet initiation, and shock and detonation wave focusing. Requirements for an initiation device for PDEs include: low energy, short length, and minimal flow obstruction.

DDT

Deflagration-to-detonation transition (DDT) is a mechanism of interest for use in practical engine design. However, current practice in designing detonation initiation systems using DDT is highly empirical and no design guidelines are available. A study of DDT initiation was performed for various fuels with oxygen and diluents[1]. The time required for detonation was measured as a function of initial conditions and correlated with the detonation and deflagration characteristics of the mixture.

The detonation tube used for the DDT experiments is 1.5 m long and has an internal diameter of 38 mm. The ignition source is a spark plug followed by a Shchelkin spiral. The spiral enhances transition of the spark-induced deflagration to a detonation. It is 305 mm long, has a 38 mm outside diameter, and a wire diameter of 4 mm. The distance between the coils is 11 mm. The tube is equipped with three pressure transducers spaced 400 mm apart along the length of the tube. The pressure transducers enabled the measurement of the DDT time, which is defined as the time from the spark discharge to the time at which a detonation wave reached the first pressure transducer. A successful DDT event occurred if the wave propagated within +1% and –2% of the Chapman-Jouguet (CJ) detonation velocity from the first pressure transducer through the remainder of the detonation tube.

Experimental results are presented on Figure 1. Multiple data points at the same condition indicate repeat experiments. DDT time data vs equivalence ratio in hydrogen-oxygen are shown in

Figure 1a. The familiar U-shaped behavior is observed with minimum DDT times occurring near the stoichiometric condition. At stoichiometric conditions, DDT times are greatest for propane, followed by hydrogen. The shortest DDT times are observed in ethylene. DDT times decrease with increasing pressure and the same hierarchy between fuels is maintained. Increasing the dilution increases the DDT time. Carbon dioxide was found to be the more effective inhibitor of the DDT process, followed by nitrogen, helium, and argon. Repeat experiments showed that the data followed a fairly normal statistical distribution, with temporal deviations around the mean of approximately ±5%.

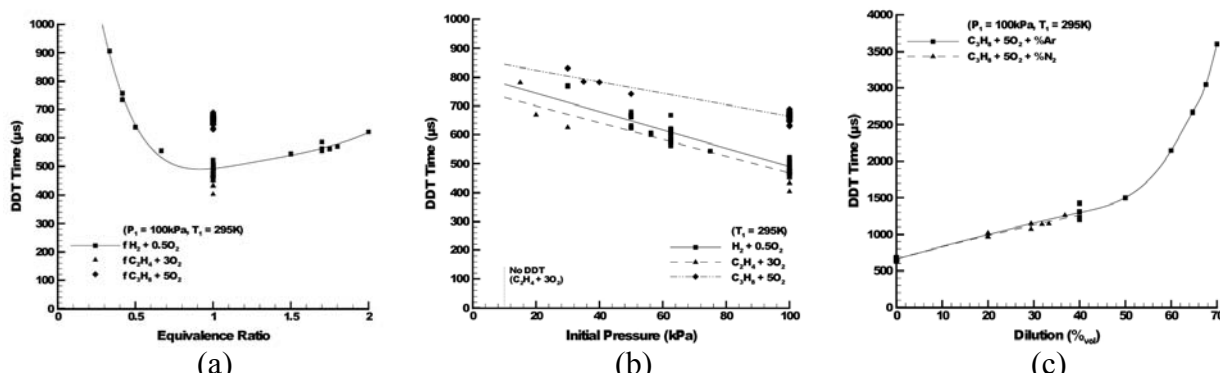(a)　　　　　　　　　(b)　　　　　　　　　(c)

Figure 1. DDT time as a function of initial conditions for fuel-oxygen mixtures. a) DDT time vs equivalence ratio. b) DDT time vs initial pressure. c) DDT time vs percent dilution for propane-oxygen mixtures.

DDT times (t_{DDT}) were analyzed in terms of deflagration and detonation characteristic properties. In particular, characteristic times can be associated with ideal instantaneously-initiated detonations ($t_{CJ}=L/U_{CJ}$) and laminar flames ($t_{lam}=L/V_f$), where L is the distance from the spark plug to the first pressure transducer, U_{CJ} is the CJ detonation velocity, and V_f is the flame propagation speed, equal to the product of the burning velocity and the expansion ratio of the mixture. The time required for the acceleration and transition process is given by the excess transit time $(t_{DDT}-t_{CJ})$. Since the acceleration process is much slower than the detonation onset process, we expect the excess transit time to be dominated by the time required for flame propagation within the spiral and the excess transit time to be proportional to the laminar flame propagation time. In general, the results will be a function of the geometry and mixtures parameters such as expansion ratio, σ, Lewis number, Le, and Zeldovich number, β. Non-dimensional DDT times, $(t_{DDT}-t_{CJ})/t_{lam}$, are shown on Figure 2. All non-dimensional DDT times fall in a narrow range between 0.06 and 0.09. The modest range of variation indicates that our scaling ideas capture the essential dependence of the DDT time on the characteristic idealized time scales.
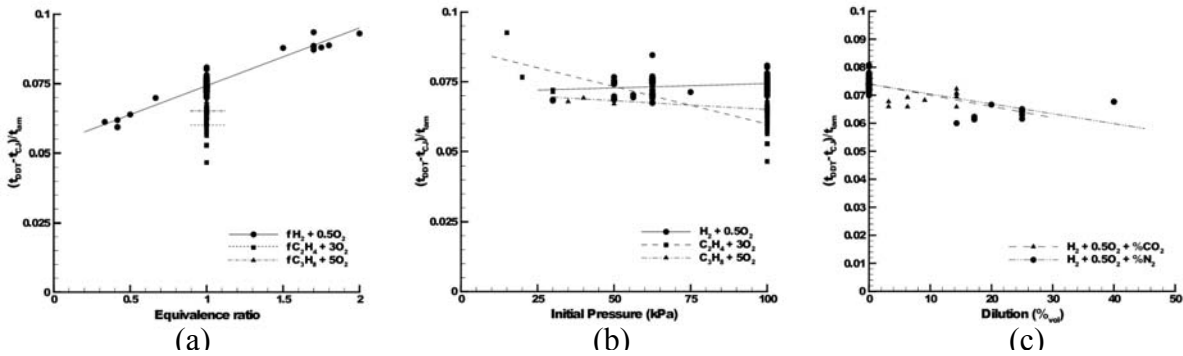
Figure 2. Non-dimensional DDT for fuel-oxygen mixtures. a) vs equivalence ratio. b) vs initial pressure. c) vs dilution for hydrogen-oxygen mixtures.

We attempted to correlate the non-dimensional DDT times with other non-dimensional flame parameters, such as the expansion ratio or the Zeldovich number. Figure 3 shows correlations with σ and $\beta(Le-1)$. The expansion ratio represents how much a fluid particle will expand when it combusts. It is therefore expected that mixtures with higher expansion ratios will be more susceptible to DDT. The combination $\beta(Le-1)$ is expected to control the onset of cellular instability in flames. Unstable flames are expected to accelerate faster than stable flames. In general, large expansion ratios and small Lewis numbers are conducive to minimizing DDT time. No special influence of the Zeldovich number was identified in this study. Further work with a large range of values will be required in order to isolate the role of this factor.
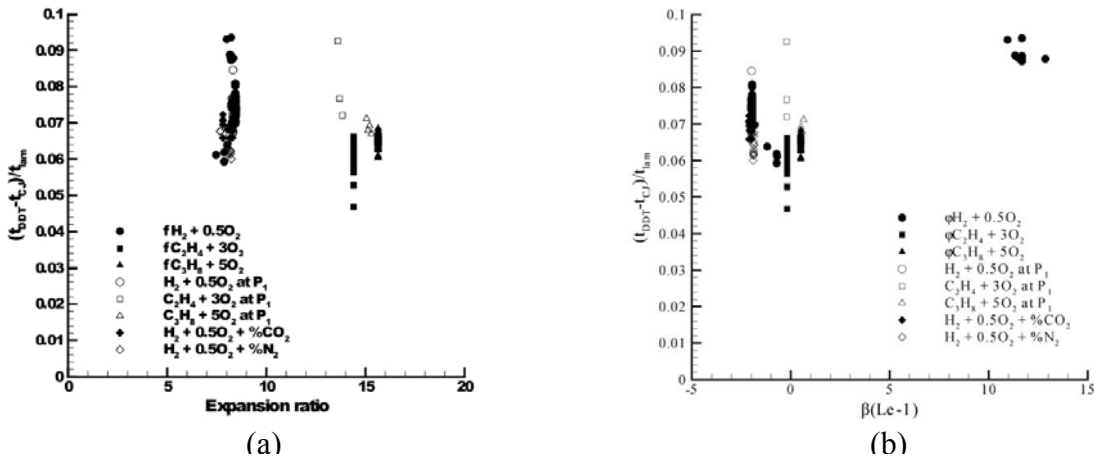

Figure 3. Non-dimensional DDT time correlation. a) DDT time vs expansion ratio. b) DDT time vs $\beta(Le-1)$.

Hot Jet Initiation

The effectiveness of using a hot turbulent jet to initiate a detonation in a short distance was investigated experimentally[2]. A turbulent jet of combustion products, passing from a driver section through an orifice into a test section, was used to initiate a turbulent flame in the test gas. The turbulent flame may transition to detonation. Such low-energy methods of detonation initiation are of particular interest to PDEs.

3

The experiments were performed in the ballistic pendulum facility with a tube that consists of two vessels: a 100 cm^3 volume driver section and a 1 m long by 76.2 mm diameter test section. The vessels are connected by an orifice, the diameter of which can be varied. The test section is equipped with three pressure transducers and ten ionization probes to measure the pressure history and wave velocity. The driver section has a pressure transducer on the ignition end wall. The driver is filled with a stoichiometric propane-oxygen and the test section is filled with stoichiometric propane-oxygen mixture with varying nitrogen dilution. A Mylar diaphragm initially separates the driver and test gases. The aim of the current study is to examine the effect of the orifice diameter and the initial pressure of the driver section on the maximum (or critical) nitrogen dilution for which a detonation can be initiated in the test section.

Driver pressure is found to have a mild effect on the critical N_2 dilution, see Figure 4. Increasing the driver pressure by a factor of four resulted in an increase in the critical N_2 dilution from 30% to 40%. Figure 5a shows the effect of varying the orifice diameter on the critical N_2 dilution with the initial driver pressure at 1 bar. Increasing the orifice diameter from 3 mm to 19 mm increases the critical dilution level from 30% to 40% N_2. Figure 5b shows measured I_{sp} vs test section N_2 dilution for initial driver pressures of 1 to 4 bar. The orifice diameter is 3.125 mm. The solid line corresponds to the theoretical impulse model proposed by Wintenberger et al.[23] Experiments were also carried out with an array of orifices to examine the role of jet mixing. For a given open area, the multiple hole geometry resulted in a 5% increase in the critical dilution level over the equivalent single hole geometry.
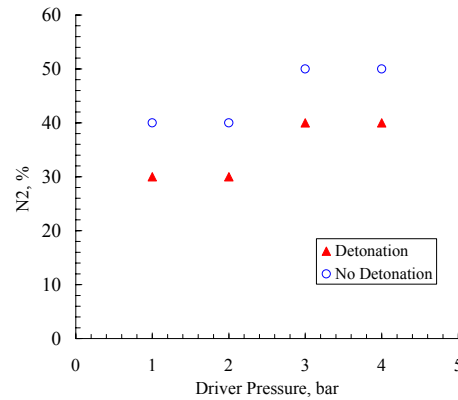

Figure 4. Critical N_2 dilution amount vs initial pressure in the driver section.
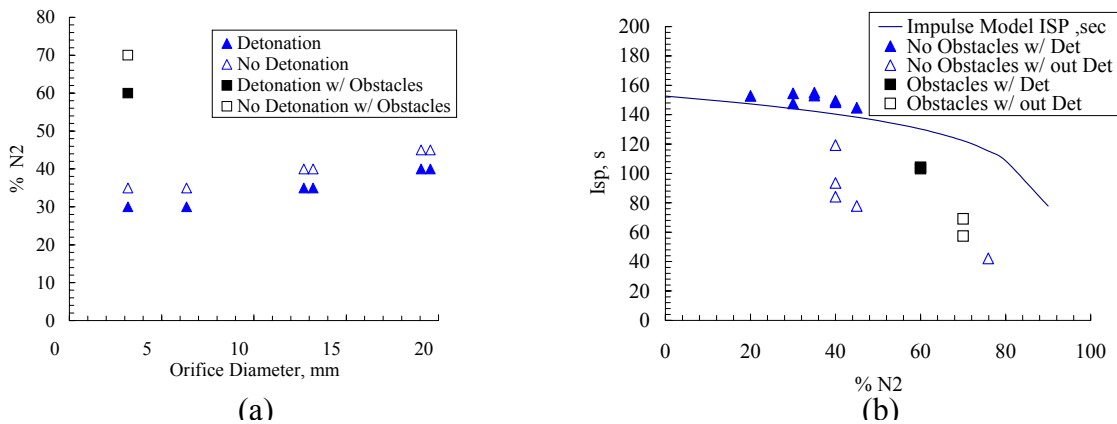

(a)

(b)

Figure 5. a) Critical N_2 dilution amount vs orifice diameter. b) Corresponding I_{SP} measurements.

Basic Studies of Shock Focusing

Shock wave focusing is a method that can be used to initiate detonations in insensitive mixtures and has a low energy input requirement. Shock wave focusing involves the collision of two or more shock waves. In the region behind the colliding shock waves, high pressures and temperatures occur. In general, increased temperatures and pressures facilitate the initiation of detonation. We examined the characteristics of the focal region in order to develop criteria for the initiation of detonations under these conditions.

The study was performed by using numerical simulation to examine shock focusing in non-reactive mixtures and making comparisons with previous results. The results of several simulations are shown and compared to experimental data in Figure 6. Pressure and temperature amplifications were found to be very sensitive to the type of reflection. Three types of reflection are observed and were characterized as a function of the incident wave strength and the reflector geometry. Type A reflection is characterized by the formation at focusing of a strong Mach stem growing with time, leaving an open focal region. This reflection type occurs for strong shocks and shallow reflectors. Type B reflection occurs when the diffracted shocks at the reflector edges intersect on the axis after focusing and then precede the Mach stem. Type C reflection occurs when the diffracted shocks at the reflector edges intersect on the axis before focusing. It results in a closed focal region, a small triangular region of fluid that is compressed by focusing. This reflection type is characteristic of weak shock waves and deep reflectors. A summary of the reflection regimes is given in Figure 7. Type C reflection was found to produce higher pressure and temperature amplification; however, this amplification is usually followed by a very strong expansion.
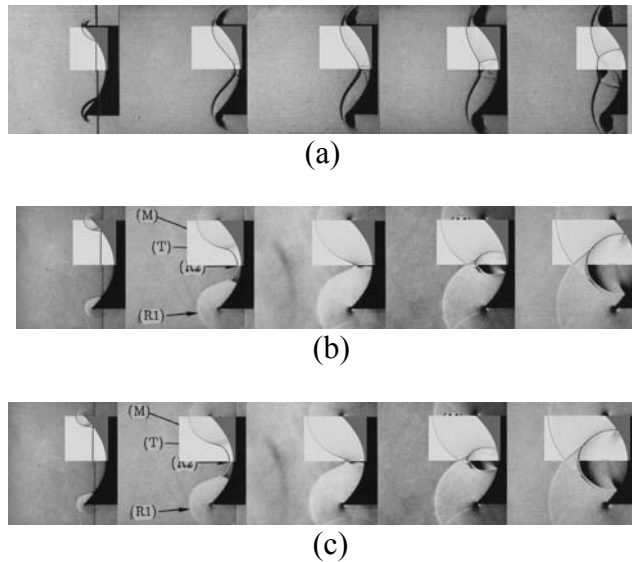

(a)

(b)

(c)

Figure 6. Numerical simulations of shock wave focusing using Amrita[3] and comparisons with previous experimental results of Izumi et al[4].
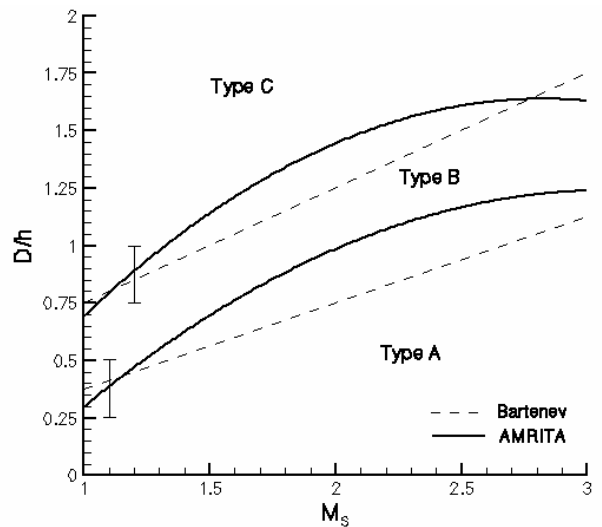
Figure 7. Map of focusing regimes as a function of reflector geometric parameters (D/h is the depth-to-half-height ratio) and incident shock Mach number M_s. Comparison between CFD (Amrita[3]) and previous studies (Bartenev et al.[5]).

Wave Shaping

Efficient methods of initiating detonations in insensitive fuel-air mixtures (such as JP10 and air, or propane and air) are of interest for air-breathing PDE applications. A necessary step in moving from laboratory demonstration to actual propulsion systems is the development of a device capable of efficiently generating the pressures and temperatures necessary to initiate detonations in these mixtures. It is desirable to develop a system capable of initiating detonations in hydrocarbon-air mixtures with a low-energy spark (less than 100 mJ) for use in short length, small diameter detonation tubes. The use of low spark energy eliminates the possibility of direct initiation of detonations in the mixtures of interest. Previous work in our group has investigated the potential of several initiation concepts which involve low-energy input, such as DDT, use of driver tubes, and wave focusing techniques. Each concept was evaluated for use with air-breathing PDEs. One such concept involves detonation wave focusing. In detonation wave focusing, a toroidally-collapsing detonation wave generates a high-pressure and -temperature focal region by adiabatically compressing products as they flow into an ever-decreasing area. The compression increases the post-detonation wave pressure higher than the CJ pressure, which results in an accelerating detonation wave.

The following sections describe a program[7] designed to maximize transmission efficiency by generating high-energy density regions via an imploding toroidal detonation wave. First, research was conducted on detonation propagation through small tubes. This determined the minimum tube diameter (and thus gas volume) necessary to propagate stable detonation waves. Second, a device capable of generating a planar detonation wave was developed to verify that several detonation fronts initiated from a weak spark and propagated though small tubes could be merged to create a detonation wave with a planar front. Finally, a low-drag initiator system capable of producing a repeatable, high-pressure focal region with a minimum amount of driver gas was built using experience gained from small tube and planar initiator data.

Small tubes

In order to minimize the amount of sensitive driver gas used in detonation initiators, the initiator volume should be as small as possible. However, as the length scale of the initiator approaches the order of the cell size of the mixture, losses due to boundary layer effects can become significant. Such losses can cause the detonation wave to fail or weaken it enough to interfere with the operation of the initiator. Thus, knowledge of minimum tube diameters and minimum initial pressures necessary to avoid severe boundary layer effects is crucial for design of an efficient system.

Researchers such as Manzhalei[6] have identified and characterized modes of detonation propagation through small tubes in acetylene-oxygen mixtures. However, limited information is available on the regime of stable propagation in propane mixtures. It was necessary to carry out experiments to establish the stable detonation regimes in propane-oxygen in order to optimize the initiator design.

A detonation wave was initiated in a driver tube and propagated into a small tube test section. The small tube test section was equipped with three pressure transducers for velocity and pressure measurements. Test sections of 1.27 mm and 6.35 mm inner diameters were used. Propane-oxygen mixtures were tested, varying the initial pressure and equivalence ratio. Data indicated that significant (>10%) velocity deficits were present when the ratio of induction distance to tube radius was greater than 0.1. This corresponds to a minimum tube diameter of 1.27 mm for stoichiometric propane-oxygen mixtures at 1 bar.
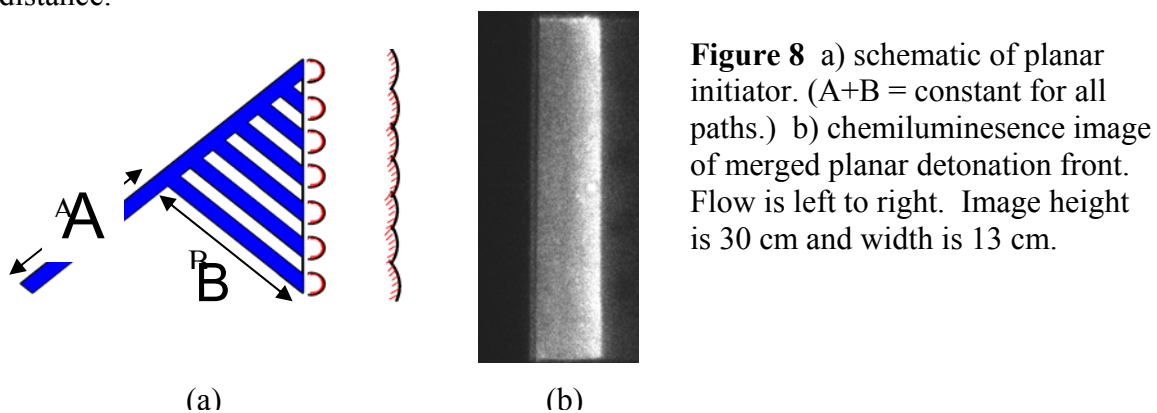
The experiments determined the minimum tube diameter necessary to propagate a detonation through a straight, unobstructed tube. The inclusion of corners, bifurcating channels, and other geometries likely to promote detonation diffraction necessitates larger tube diameters in order to ensure successful detonation propagation.

Planar Initiator

A device capable of producing a planar detonation wave was successfully built and tested to demonstrate the principles of merging a series of wave fronts into a single front. This device served as a stepping-stone in the development of the toroidal wave generator discussed below. The planar initiator is capable of producing a large aspect ratio, planar detonation from a weak spark ignition source.

The planar version, shown in Figure 8, consists of a main channel with secondary channels branching off the main channel. All secondary channels terminate on a line and exhaust into a common test section area. The channel geometry is such that all path lengths from the spark point to the secondary channel termination line are equal. For use with propane-oxygen mixtures, the main channel width was 9.53 mm and the length was 0.431 m. The width of the secondary channels was 5.08 mm and the secondary channel spacing was 2.54 mm. All channels were square in cross-section. The channels exhausted into a test section 0.305 m wide and 0.152 m long. The test section contained a ramp near the secondary channel exhaust that enlarged the channel depth from 5.08 mm to 19.05 mm over a distance of 38.1 mm. The device was filled from a reservoir with premixed propane-oxygen or ethylene-oxygen mixtures. A spark plug and associated discharge system with 30 mJ of stored energy was used to ignite the combustible mixture.

The presence of obstacles in the main channel promoted DDT, resulting in a detonation that travels down the main channel with small fronts branching off and traveling down the secondary channels. All detonation fronts exhaust into the test section at the same time and combine to form a planar detonation front. Images and pressure traces show that the device produces planar waves with deviations of less than 1 mm over the width of the test section. The results are extremely repeatable. A chemiluminescence image of the detonation front is shown in Figure 8. The planar initiator allows for efficient generation of planar detonation waves with large aspect ratios over a short distance.

Figure 8 a) schematic of planar initiator. (A+B = constant for all paths.) b) chemiluminesence image of merged planar detonation front. Flow is left to right. Image height is 30 cm and width is 13 cm.

(a)   (b)

Toroidal Initiator

To create a toroidal wave, the planar initiator design was modified such that the exit of each channel lies on a circle with the channels exhausting inwards. This involved mapping the planar design onto a cylinder, creating an annular imploding wave instead of a planar wave as shown in Figure 9. The mapping transforms the metal substrate containing the channels into an inner sleeve

while the cover plate becomes the outer sleeve. A pressure seal between the inner and outer sleeves was created by a shrink fit. All initiator channel dimensions are similar to that of the previously described planar initiator. The small channels exhaust into a test section that is 76.2 mm in diameter. The design allows the initiator to be incorporated into the walls of a PDE. Since no part of the initiator is inside the flow path, drag losses are expected to be minimal in PDE applications.

Testing was performed in stoichiometric propane-oxygen mixtures initially at 1 bar. The device was filled using the method of partial pressures. The mixture was circulated to ensure homogeneity using a bellows pump which limited initial pressures to 1 bar or greater. Pressure history was obtained at locations near the focus of the collapsing torus by four pressure transducers, one of which was placed as close to the implosion axis as possible. The distance separating the pressure transducer axis from the implosion center was 19.05 mm. The transducers were equally spaced 10.7 mm apart on a radial line with the central transducer located on the central axis of the initiator tube. A typical set of pressure traces is shown in Figure 10. Images of the detonation front luminosity were also obtained. A series of images of the collapsing detonation wave are shown in Figure 11.

The outermost three pressure transducers show a gradually decreasing pressure wave as the radius of the imploding torus decreases. The central pressure transducer, however, recorded a value above its maximum reliable operating range. This value was four times larger than the CJ pressure for the mixture. Images of the detonation front show a fairly regular collapsing toroidal wave. A structure behind the wave is also visible and may be due to the detonation interacting with the window.
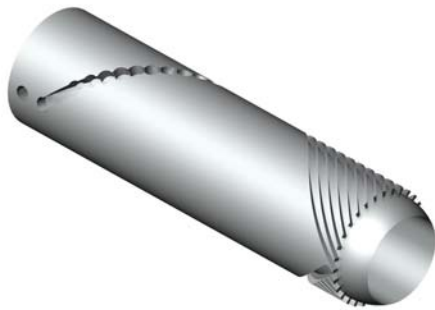

Figure 9. Schematic of annular detonation wave initiator. (Covering shell omitted for clarity.)
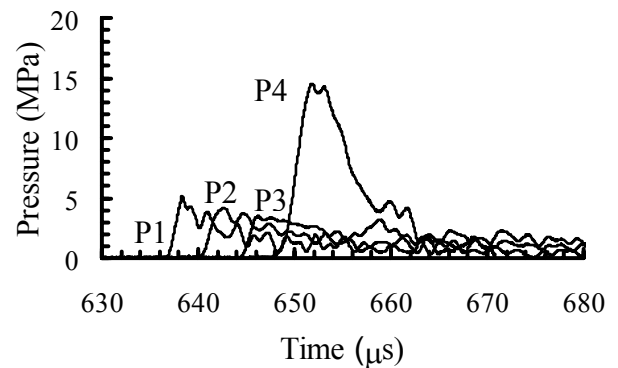

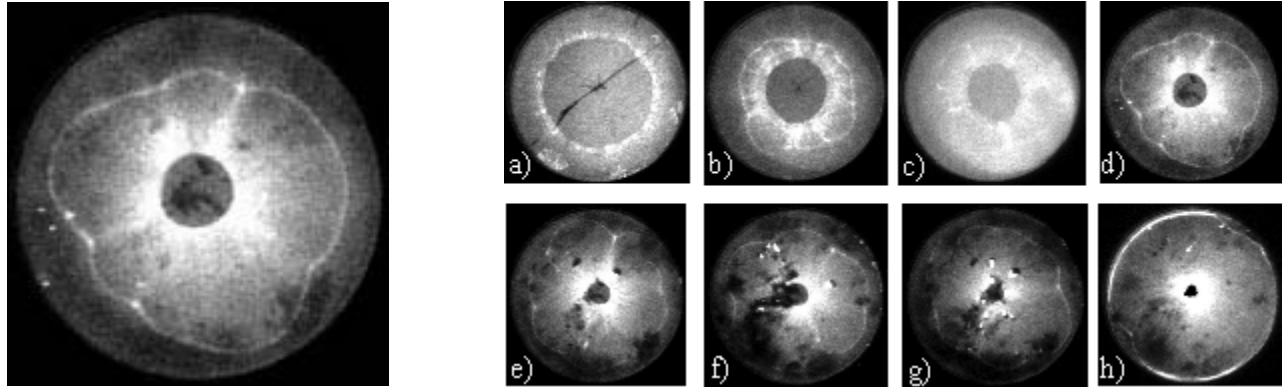**Figure 10.** Pressure traces from annular initiator tests.

Fig. 11. Chemiluminescence images of imploding detonation wave. Irregular secondary wave is thought to be due to interaction with window.

Detonation Propagation

JP10 Vapor Pressure Measurement

JP10 vapor pressure measurements were carried out to obtain reliable data for use in JP10 detonation experiments. The experimental facility was similar to that used in previous[31] vapor pressure measurements in Jet-A. A vessel containing liquid JP10 was placed in an ethylene glycol bath. The ethylene glycol temperature was regulated by a feedback-controlled heating system. Thorough mixing of the ethylene glycol and insulation of the bath ensured a unifrom temperature distribution. The temperature was set using a digital controller and measured using thermocouples in the bath and in the test liquid. The temperature was varied from ambient to 120°C.
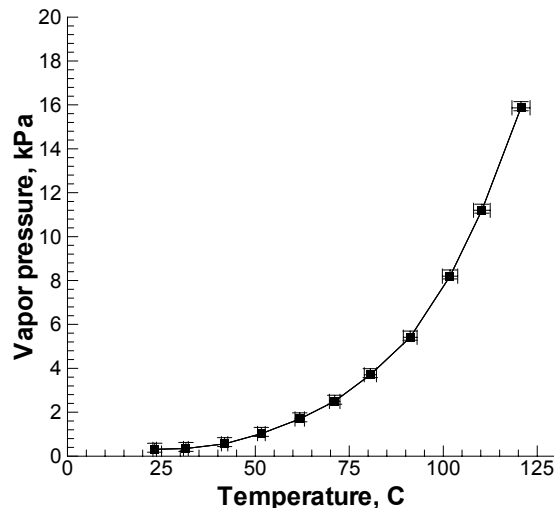

Figure 12. Measured vapor pressure of JP10.

The vapor pressure of JP10 was measured in steps of 10°C using a digital pressure gauge. At every step, pressure measurements were taken only after ensuring that the temperature of the bath and the test liquid was stable. The vessel was then evacuated at the start of the experiment and at each temperaure, the pressure was allowed to build up to a constant value before the pressure was recorded. The results are plotted on Figure 12. The error bars represent the uncertainties in the

measurements, which are ±2% for the temperature and –0.13/+0.28 kPa for the measured pressure, accounting for gauge precision and leak rate.

PDE Fuel Characterization

Liquid hydrocarbons are the fuel of choice for aviation propulsion systems, including the PDE. Much of the published PDE research to date has used low molecular weight hydrocarbon fuels (C_1-C_3) due to the difficulty of creating uniform fuel-air mixtures with liquid hydrocarbon fuels and initiating detonations in these mixtures. The detonation cell width, defined as the average transverse wave spacing recorded on a sooted foil (Figure 12), is a useful measure of the sensitivity of a mixture to detonation. Generally speaking, the smaller the cell width, the smaller the minimum energy required to initiate detonation. The cell width can also be empirically related to other dynamic parameters such as the minimum tube diameter that is required for detonation propagation.

During the course of this program, the Caltech 280 mm detonation tube was modified to include a heating system and strengthened to extend the range of operation with liquid fuels and higher oxygen concentrations. The cell widths in vaporized JP10 have been measured at temperatures above 80°C for several mixtures[8]: a) JP10-air at 100 kPa for equivalence ratios between 0.7 and 1.4 (Figure 13). b) stoichiometric JP10-O_2 and JP10-air for initial pressures between 20 and 130 kPa (Figure 14) c) JP10-O_2-N_2 at an equivalence ratio of one and nitrogen amounts between zero and air equivalent (Figure 15). The cell widths of JP10 mixtures were found to be comparable to those of propane and hexane mixtures. This result suggests that propane may be a useful surrogate fuel for preliminary PDE studies.
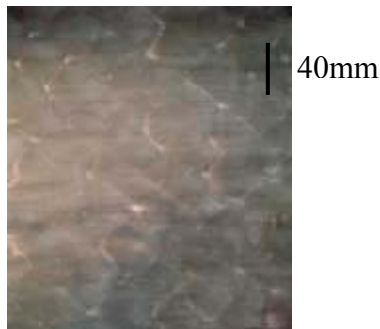

Figure 13. Soot foil of JP10-20%C_2H_2-Air. Detonation propagated from left to right.
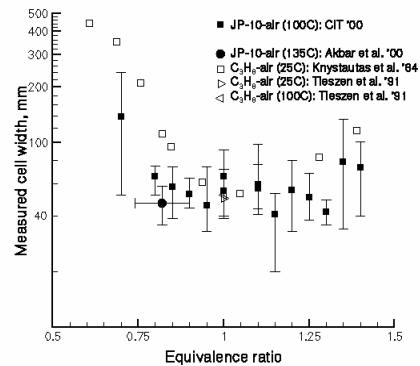

Figure 14 Detonation cell width measurements in JP10-Air vs equivalence ratio. Propane data are shown for comparison
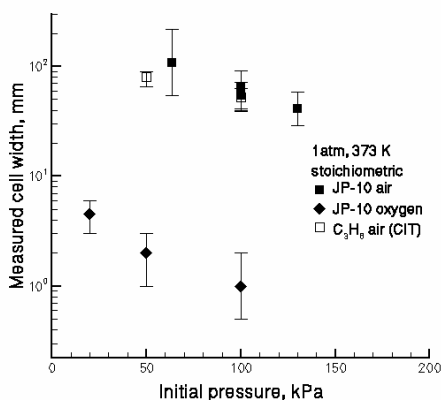
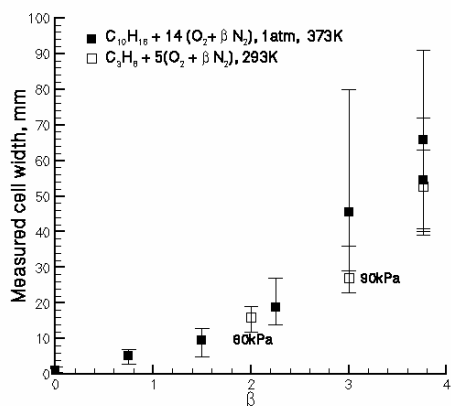**Figure 15.** Cell width measurements in JP10-air with varying initial pressure.

Figure 16. Cell width measurements in JP10-O_2 with varying nitrogen dilution to JP10-air.

The addition of hydrocarbon fuels to JP10 was investigated (Figure 17). C_2H_2, C_2H_4, and CH_4 were chosen as examples of low-molecular weight hydrocarbons that result from thermal or catalytic decomposition[9] of JP10. Such data will also be of use in validation studies for JP10 reaction mechanisms.
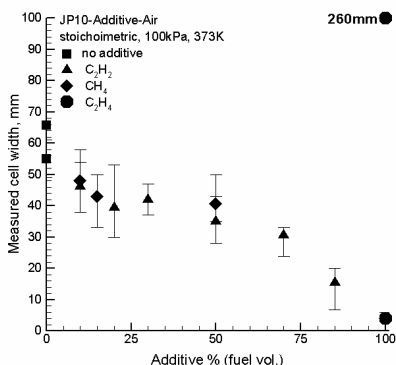

Figure 17. Detonation cell width measurements in JP10-hydrocarbon-air at 100 kPa initial pressure, 353 K initial temperature. All data points for hydrocarbon-air are from Tieszen et al. 1991[10]. CH_4-Air cell width is actually 260mm.

Detonation structure

Several important areas of PDE development such as initiation, minimum tube size, and tube geometry benefit from greater understanding of the fundamental mechanism by which detonation waves propagate. The cellular nature of all detonation waves propagating near the CJ velocity is well known and may be observed from tracks on sooted foils, as discussed above. Previous researchers[11,12,13,14] have also used schlieren and interferometry to visualize shocks in the detonation front but resolved experimental images of chemical species in the reaction zone have been lacking.

Planar Laser Induced Fluorescence.

A dye-laser and optical system were purchased and integrated with existing equipment, cameras and an excimer laser, to create a Planar Laser Induced Fluorescence (PLIF) capability. We were able to successfully visualize OH fluorescence and carry out simultaneous schlieren visualization on detonation waves propagating H_2/O_2/diluent (N_2 and Ar) in a 150 mm by 150 mm test section[15]. Characteristic "keystone" structures in the OH intensity have been revealed and correlated with detonation wave instability structures computed on the basis of reduced chemistry and also inferred from gas dynamic considerations. A marked difference in structure is observed between nitrogen

and argon diluted mixtures, which agrees with the known characterization of the cellular structures as irregular and regular, respectively[16].
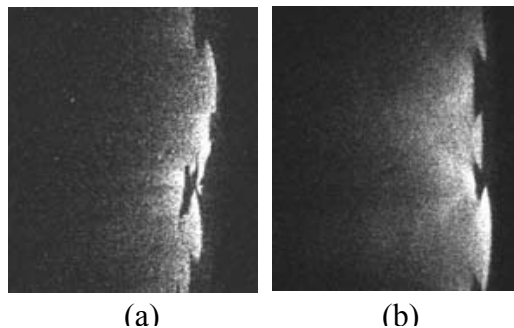

Figure 18. OH PLIF images of reaction zone structure in $2H_2$-O_2-$4.5N_2$ (a) and $2H_2$-O_2-$17Ar$ (b) at 20 kPa.

(a)   (b)

In the current experimental setup, three-dimensional effects complicate both schlieren and PLIF images. An investigation was made of the possibility of simplifying the flow field by damping out-of-plane transverse waves using a porous wall. The technique was found to be successful, but only for a limited range of mixtures. The experiments also studied detonation propagation through narrow channels of different widths. Diagnostics included soot foils to record cell structure and pressure gauges to measure velocity deficits.
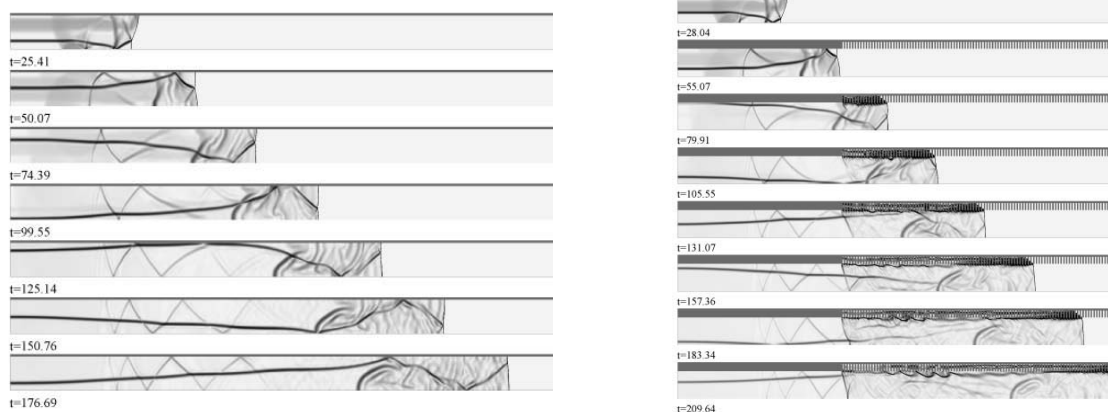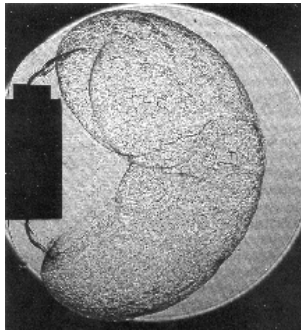

Figure 19. AMRITA[3] simulations of a Mach stem propagating over solid and porous walls by Prof. H.G.Hornung, Caltech. The transverse wave is damped on reflection from the porous surface.

Figure 20. Soot foil obtained in 18 mm channel with porous wall in $2H_2$-O_2-$3Ar$, 30kPa. The detonation propagated left to right. Triple point tracks are significantly weakened downstream of the porous wall (far right), corresponding to damped transverse waves.

Detonation Diffraction

Diffraction of detonations in H_2, C_2H_4, and C_3H_8 in O_2/diluent from a 38-mm orifice into a 150 mm by 150 mm test section[17] has been investigated. Single-frame laser schlieren, rotating-mirror framing, and chemiluminescence images have been used to develop an analytical model of critical conditions for detonation diffraction. The model uses a detailed reaction mechanism validated against experimental shock tube data from a wide variety of sources. Excellent quantitative agreement has been obtained between experimental and computed critical tube diameters.

(a)   (b)

Figure 21. a) Laser shadowgraph image of detonation diffraction in the critical regime. b) Experimental critical diameter data vs. model prediction.

Direct Measurements of Impulse

Impulse per cycle is one of the key performance measures of a PDE.   In order to evaluate the performance of the engine concept, it is necessary to have reliable estimates of the maximum impulse that can be obtained from the detonation of a given fuel-oxidizer combination at a specified initial temperature and pressure. While the overall performance of an engine will depend strongly on a number of other factors such as inlet losses, nonuniformity of the mixture in the detonation tube, and the details (nozzles, extensions, coflow, etc.) of the flow downstream of the detonation tube exit, conclusive studies investigating the impulse available from a simple detonation tube are essential.

Direct impulse measurements were carried out[18] using a ballistic pendulum arrangement for detonations and deflagrations in a tube closed at one end (Figure 22). Three tubes of different lengths and inner diameters were tested with stoichiometric propane- and ethylene-oxygen-nitrogen mixtures. Results were obtained as a function of initial pressure and percent diluent. Experimental results were compared to predictions from an analytical model[23] and generally agreed to within 15%. The effect of internal obstacles on the transition from deflagration to detonation was studied. Three different extensions were tested to investigate the effect of exit conditions on the ballistic impulse for stoichiometric ethylene-oxygen-nitrogen mixtures as a function of initial pressure and percent diluent.

Figure 22. Schematic and photograph of ballistic pendulum experiment.

All mixtures were ignited by a spark with a discharge energy (30 mJ) much less than the critical energy required for direct initiation of a detonation (approximately 283 kJ for propane-air mixtures[19] and approximately 56 kJ for ethylene-air mixtures[19] at atmospheric conditions). Thus, detonations were obtained only by transition from an initial deflagration. The presence of a

deflagration is denoted by a gradual rise in the pressure histories as the unburned gas ahead of the flame is compressed due to the expansion of the burned gases behind the flame. If the correct conditions exist, this initial deflagration can transition to a detonation wave. Otherwise, transition will not occur and the deflagration wave will travel the entire length of the tube.

Direct impulse measurements for propane- and ethylene-oxygen-nitrogen mixtures were made with different obstacle geometries. Figure 23 shows impulse as a function of diluent amount for the 0.609 m tube with Shchelkin spiral obstacles. It can be seen that the obstacles with a smaller pitch have a lower impulse than those with a larger pitch. We attribute this loss in impulse as being due to a greater form drag associated with the flow around the obstacles as the spiral pitch decreases. At 100 kPa, a 5% reduction in the distance between successive coils causes a 13% reduction in impulse if the spirals extend over the entire tube length. In Figure 24, we show impulse for blockage and orifice plate obstacles. Although obstacles can induce DDT in less sensitive mixtures and significantly increase the impulse, the obstacle drag can decrease the impulse by an average of 25% from the value measured without obstacles when fast transition to detonation occurs. When obstacles are present, the impulse obtained from integrating the thrust wall pressure history significantly overpredicts the actual impulse.
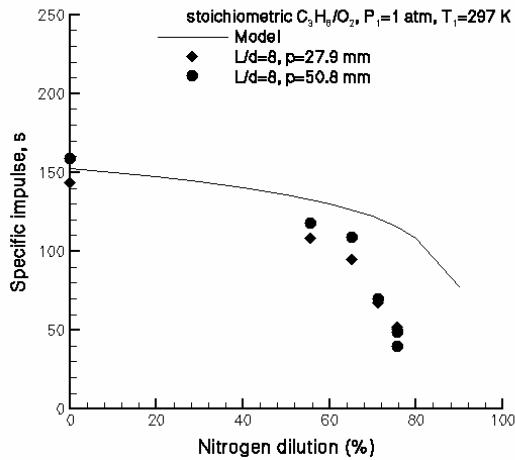

Figure 23. Measured impulse vs. N_2 dilution for different spiral geometries.
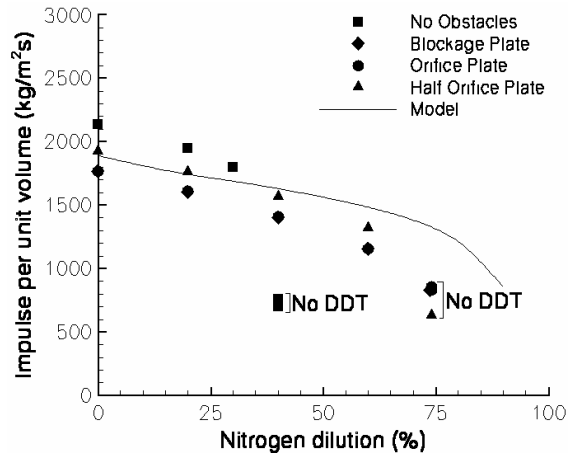
Figure 24. Measured impulse vs. N_2 dilution for orifice and blockage plates.

From Figure 24, it can be seen that, without obstacles, detonation cannot be achieved in this tube for nitrogen dilutions of 40% or greater. A dramatic drop in measured impulse occurs for these mixtures. The addition of obstacles enabled DDT to occur in mixtures with up to 60% nitrogen dilution. Deflagrations propagate slowly through the tube, compressing the unburned gas ahead of the flame. This unburned gas compression is sufficient to rupture the thin diaphragm causing a considerable part of the mixture to be ejected outside the tube. The mixture ejected from the tube does not contribute to the impulse due to its unconfined burning. The effect of this mixture spillage due to no DDT can be seen in the cases with greater than 70% diluent where a 30-50% reduction in impulse is observed. The onset of a detonation wave can mitigate this effect if it occurs sufficiently quickly. If DDT occurs early enough in the process, the detonation can overtake the compression waves created by the deflagration before they reach the diaphragm. Cases of late or no DDT illustrate the importance of more sophisticated initiation methods for less sensitive fuels, such as storable liquid hydrocarbons (Jet A, JP8, JP5 or JP10) with cell widths similar to

propane. Experiments with more sensitive ethylene-oxygen-nitrogen mixtures show that using obstacles to induce DDT within the tube can be effective.

Effect of extensions

Proposed concepts for pulse detonation engines have often included the addition of different kinds of extensions, including nozzles, to the basic straight detonation tube. In part, this is motivated by the effectiveness of converging-diverging nozzles in conventional rocket motors. The effectiveness of a converging-diverging nozzle is based on the steady flow conversion of the thermal to kinetic energy. However, the PDE is an unsteady device that relies on waves to convert the thermal energy into kinetic energy. It is not obvious how a nozzle would affect performance since the diffraction of the detonation wave through a nozzle is a complex process that involves significant losses. We have approached this problem experimentally by examining the effect of various exit treatments on the measured impulse. In our tests, a thin diaphragm separates the tube length filled with the combustible mixture from the extension, which was filled with air at atmospheric conditions. This simulates the condition of having a single tube only partially filled with explosive mixture.

Three different extensions were tested on the detonation tube with a length of 1.016 m in a ballistic pendulum arrangement to determine their effect on the impulse. Each extension modified the total tube length, L, while the charge length, L_o, remained constant. The first extension was a flat plate ($L/L_o = 1$) or flange with an outer diameter of 0.381 m that extended radially in the direction perpendicular to the tube's exhaust flow. A hole located in the center of the plate matched the tube's inner diameter, thus increasing the apparent wall thickness at the exhaust end from 0.0127 m to 0.1524 m. The purpose of this flange was to see if the pressure behind the diffracting shock wave would contribute significantly to the specific impulse. The second extension was a straight cylinder ($L/L_o = 1.6$) with a length of 0.609 m. This extension simulated a partial fill case. The third extension was a diverging conical nozzle ($L/L_o = 1.3$) with a half angle of eight degrees and a length of 0.3 m.

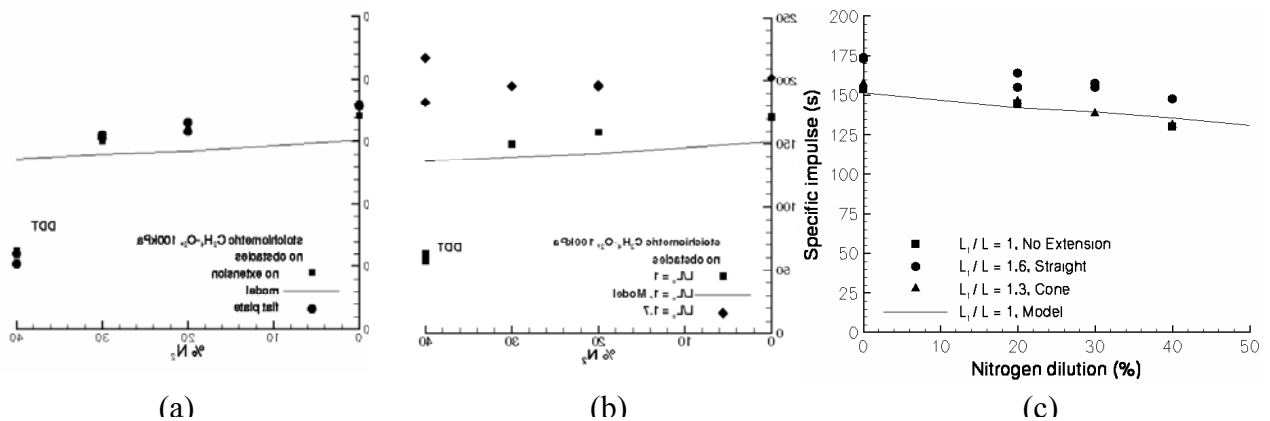(a)   (b)   (c)

Figure 25. Effect on measured impulse of different tube exit geometry.

The flat plate and straight extension were tested with ethylene-oxygen-nitrogen mixtures in a tube that did not contain internal obstacles (Figure 25 a and b). The flat plate extension yielded a

maximum specific impulse increase of 5% at 0% nitrogen dilution which is within our uncertainty in measured impulse. This effect can be understood by recognizing that the flat plate or flange extension has a minimal effect on the impulse since the shock Mach number decays very quickly as the shock diffracts out from the open end. The straight extension increased the measured specific impulse by 18% at 0% nitrogen dilution, whereas a 230% increase in the specific impulse was observed at 40% nitrogen dilution. This large increase in the specific impulse occurred since the additional tube length enabled DDT to occur in the extension's confined volume.

To better isolate the effect of the extensions over the range of diluent percentages tested, cases of late or no DDT were eliminated by the addition of obstacles over half the tube length (Figure 25c). The straight extension attached to a tube with internal obstacles increased the specific impulse by an average of 13%. As shown above, the straight extension attached to a tube without internal obstacles increased the impulse by 18%. This 5% reduction in impulse is due to drag and heat transfer losses induced by the obstacles. The diverging nozzle had a minor effect, increasing the specific impulse by an average of 1%, which is within the experimental uncertainty.

The straight extension was more effective than the diverging nozzle in increasing impulse (Figure 25c). One explanation[20, 21] of this effect is that the additional length of the straight extension as compared with the diverging extension delays the arrival of the expansion wave from the tube exit, effectively increasing the pressure relaxation time and the impulse. Standard gas dynamics considerations indicate that two reflected waves will be created when an extension filled with inert gas is added to a detonation tube. The first wave is due to the interaction of the detonation with the mixture-air interface and is much weaker than the second wave created by the shock or detonation diffraction at the tube exit. Additionally, the continuous area change of the diverging nozzle creates expansion waves that propagate back to the thrust surface resulting in a gradual but continuous decrease in pressure that starts as soon as the detonation reaches the entrance to the diverging nozzle. Another way to interpret these impulse results with extensions is that the added inert gas provides additional tamping[22] of the explosion which will increase the momentum transfer from the detonation products to the tube.

The results of this experimental work have several significant implications for PDE technology. The use of internal obstacles may be effective in initiating detonations in highly insensitive mixtures of larger cell widths such as all the storable liquid hydrocarbon fuels. However, because there are limits to obstacle effectiveness, their use will have to be optimized for a given mixture and application. The use of extensions may also be beneficial in augmenting the specific impulse obtainable from a given fuel-oxidizer mass. However, the maximum impulse is always obtained by filling the available tube volume entirely with the combustible mixture. Additional studies in progress are required to quantify the effect on impulse that could be obtained with diverging and converging-diverging nozzles[23].

Analytical Modeling of Impulse

A key issue in evaluating pulse detonation engine performance is reliable estimates of the performance as a function of operating conditions and fuel types. It is therefore desirable to develop simple analytical methods that can be used to rapidly and reliably estimate the impulse delivered by a detonation tube during one cycle. An analytical model for the impulse of a single-cycle pulse detonation tube has been developed and validated against experimental data[24]. In developing our model, we have considered the simplest configuration of a detonation tube, a tube open at one end and closed at the other, and single-cycle operation. We realize that there are significant issues associated with inlets, valves, exits, and multi-cycle operation. However, we are anticipating that our simple model can be incorporated into more elaborate models that will take these features into

account and that the present model will provide a key component for realistic engine performance analysis.

The model is based on the pressure history of the thrust surface (closed end) of the detonation tube. An analysis of the gas dynamic processes inside the tube shows that the propagation of the detonation from the closed end to the open end of the tube is followed by the generation of a reflected expansion wave propagating back to the thrust surface, for all hydrocarbon-oxygen and hydrocarbon-air mixtures and most cases with hydrogen. After interacting with the Taylor wave, the reflected expansion propagates to the closed end of the tube, decreasing the pressure and accelerating the fluid towards the open end through a "blowdown" process. The pressure at the thrust surface is modeled by a constant pressure followed by a decay due to this "blowdown" process. The duration and amplitude of the constant pressure portion are determined by analyzing the gas dynamics of the self-similar flow behind a steadily-moving detonation within the tube. In particular, the constant pressure duration can be calculated by computing the trajectory of the first characteristic of the reflected expansion wave. The decaying part of the pressure history, corresponding to the gas expansion process, is modeled using dimensional analysis and empirical observations.
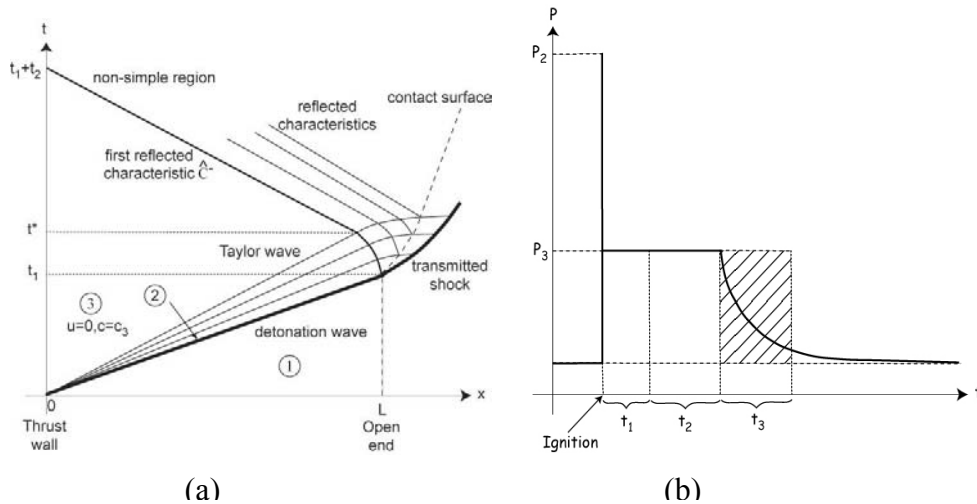

Figure 26. a) Wave diagram showing the gas dynamic processes inside the detonation tube. b) Modeling of the pressure history at the thrust surface.

(a)   (b)

The impulse model was validated against single-cycle experimental data obtained in our laboratory[18]. Direct experimental measurements were carried out using a ballistic pendulum technique. In these experiments, detonation initiation was obtained via DDT. The agreement between the model predictions and the experimental values is better for cases with high initial pressure and no nitrogen dilution. In general, the model underpredicts the experimental values for unobstructed tubes by up to 15%, and it overpredicts them for cases when obstacles are used by up to 15%. Comparisons with multi-cycle experiments[25] were also carried out for hydrogen-air and propane-air mixtures. The specific impulse predictions are fairly close to the experimental data (within 8% error for hydrogen and within 15% for propane). The decrease in experimental impulse at low equivalence ratios is probably caused by cell-size effects in the case of propane and increased transition distance in the case of hydrogen. Thrust was calculated from the single-cycle impulse predictions by assuming a very simple PDE consisting of a sequence of ideal single cycles. Comparison with multi-cycle thrust measurements[25] resulted in good agreement (within 4% error).
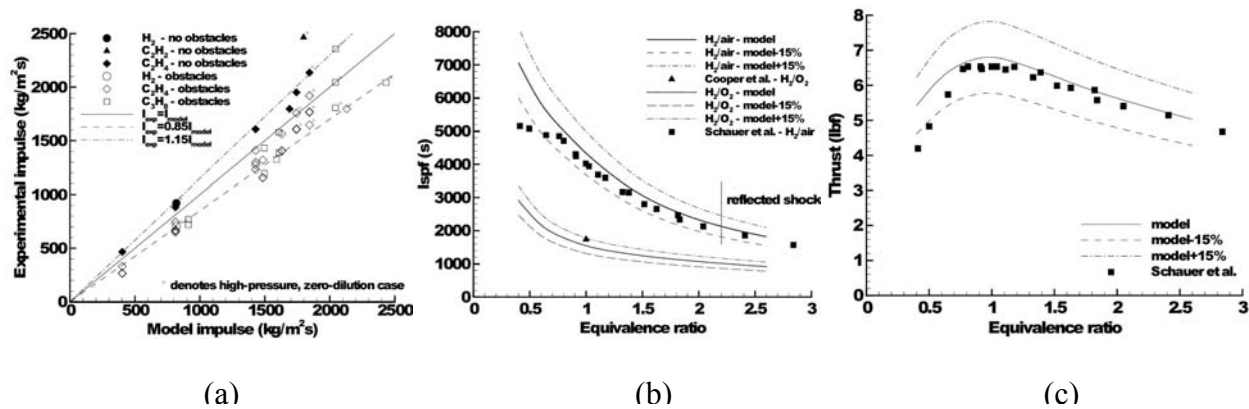
(a)	(b)	(c)

Figure 27. Comparison of model impulse with a) single-cycle experiments[18] b) multi-cycle experiments[25] and c) comparison of thrust predictions with multi-cycle experiments[25].

Impulse calculations were carried out using the model for different mixtures including hydrocarbon fuels and hydrogen, and for a wide range of initial parameters including equivalence ratio, initial pressure, and nitrogen dilution. The input required by the model consists of the outside pressure, the detonation velocity, the speed of sound behind the detonation front, the CJ pressure, and the ratio of the specific heats of the products. The impulse was calculated for the following fuels: ethylene, propane, acetylene, hydrogen, Jet A, and JP10 with varying pressure (from 0.2 to 2 bar), equivalence ratio (from 0.4 to 2.6), and nitrogen dilution (from 0 to 90%). Results were expressed in terms of impulse per unit volume of the tube, mixture-based specific impulse, and fuel-based specific impulse. The influence of the initial temperature was also investigated. The predicted values of the mixture-based specific impulse are on the order of 150 s for hydrocarbon-oxygen mixtures, 170 s for hydrogen-oxygen, and on the order of 115 to 130 s for fuel-air mixtures at initial conditions of 1 bar and 300 K. The trends observed are explained using a simple scaling analysis showing the dependency of the impulse on initial conditions and energy release in the mixture. The scaling relationships and equilibrium computations were used to verify the following conclusions:

1. At fixed composition and initial temperature, the impulse per unit volume varies linearly with increasing pressure.
2. At fixed composition and initial pressure, the impulse per unit volume varies inversely linearly with initial temperature.
3. At fixed composition and sufficiently high initial pressure, the specific impulse is approximately independent of initial pressure and initial temperature. This makes specific impulse the most useful parameter for estimating pulse detonation tube performance over a wide range of initial conditions.
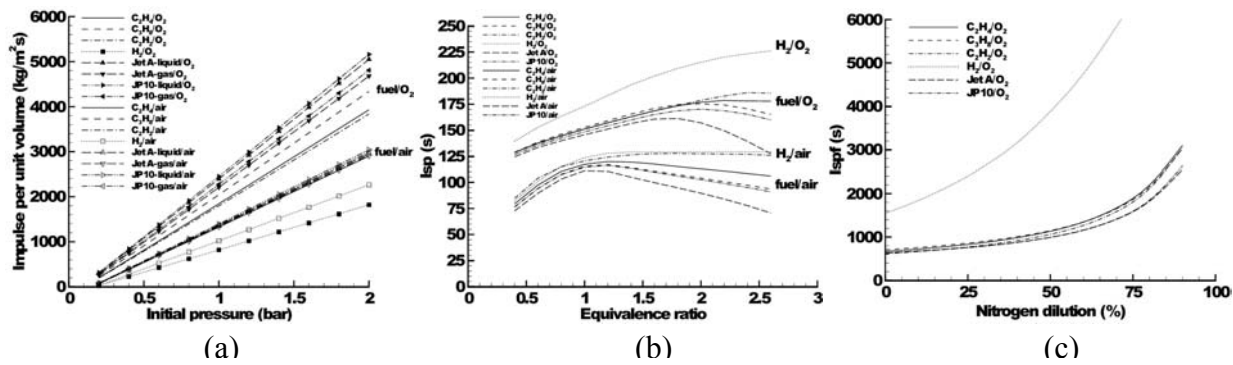
Figure 28. Impulse calculations for different fuels varying initial parameters. a) impulse per unit volume varying initial pressure (stoichiometric fuel-oxygen, 300 K). b) mixture-based specific impulse varying equivalence ratio (1 bar, 300 K). c) fuel-based specific impulse varying nitrogen dilution (stoichiometric fuel-oxygen, 1 bar, 300 K).

Tube Response to Detonation Loading

The PDE is a new kind of aerospace structure that involves many challenges in repetitive, traveling, impulsive loading and thermomechanical fatigue. Studies at Caltech have investigated different aspects of this problem. The linear elastic, plastic, and fracture response of metal tubes under single-cycle shock and detonation loading have been studied.

Elastic Response

The traditional strategy for design of tubes under shock or gaseous detonation loading is to use linear elastic static formulas and assume a dynamic amplification factor (defined as the ratio of dynamic strain to static strain of the same pressure magnitude) of two. This model may be inadequate if the true dynamic stresses are increased due to resonance or reflection effects. It is apparent that a reliable relation between the dynamic amplification factor, the load traveling speed, and the various tube parameters should be established.

The GALCIT 280-mm stainless steel detonation tube was used to verify the existence of the critical velocity phenomenon in the linear elastic regime[26]. Strain gages were mounted on the tube, which was loaded with a range of CJ detonation speeds. Amplification factors ranging from 1 to 4 were measured, with maximum strain occurring when the CJ speed reached a critical velocity that is a function of tube parameters. Analytical studies and transient finite element modeling were done and the results show fair agreement with experiments.

The critical velocity phenomenon was also verified with shock loading on a 52-mm aluminum tube [27]. Dynamic strains exceeding static strains by a factor of 3.5 were measured at the critical velocity. Again, analytical studies and transient finite element modeling were done and the results show reasonable agreement with experiments. This work shows that it is important to incorporate the critical velocity concept in shock and detonation tube designs.

Plastic Response

Our study of tubes under detonation loading was extended to the plastic regime. For these experiments, a ductile material had to be used. Copper tubes were chosen, and their plastic response under detonation loading was characterized in a series of experiments at Caltech[28]. Strains

exceeding the yield strain were obtained. The strain patterns observed were characterized by a large step-like response on which small-amplitude damped elastic oscillations are superimposed.

Fracture

      If structural failure may occur, it is desirable and often possible to have benign failure rather than catastrophic failure. The use of fracture mechanics approach in structural design allows the cracks to be brought to quick arrest and prevents fragmentation. Experiments at Caltech have shown that the fracture modes in axially preflawed aluminum tubes loaded by detonations are a strong function of the initial flaw length[29]. Different fracture modes were observed (sometimes all on the same specimen) including short distance straight propagation, helical propagation, and bifurcation.

Figure 29. Crack propagation and bifurcation under detonation loading. Detonation propagated from left to right. P_{CJ}=6.2 MPa, notch length 5.08 mm.

      It is common for flaws such as voids or cracks to develop in aerospace structures during their manufacture or lifetimes. Flaws can be small and insignificant, or they can lurk until they are fatigued to a critical size, at which point the structure fails. A fracture threshold model was developed to predict the single-cycle detonation pressure at which the tubes would burst given the tube's geometry and material properties. The experimental data showed fair agreement with the model. Strain gages were also mounted on the tubes to monitor the large scale yielding during dynamic fracture.
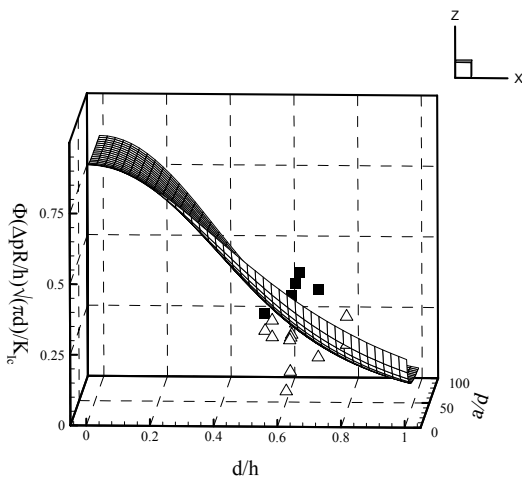

Figure 30. Fracture threshold model and experimental data. Mesh surface: theoretical threshold. Filled squares: rupture. Open triangles: no rupture.

Table 1. Nomenclature	**Table 2**. Experimental conditions

ΔP	P_{CJ}- P_{atm}
R	Tube mean radius
h	Tube wall thickness
d	Surface notch depth
2a	Surface notch length
K_{Ic}	Fracture toughness
Φ	Dynamic amplification factor

Tube material	6061-T6
Wall thickness	0.89- 1.2 mm
Tube O.D.	41.3 mm
Axial flaw length	13 to 76 mm
d/h	0.5 to 0.8
P_{CJ}	2 to 6 MPa

PDE Design Parameters.

Critical structural and performance parameters of a conceptual PDE were studied[30]. Performance parameters included thrust specific fuel consumption (TSFC), frequency limits, and thrust-to-weight ratio. The conceptual PDE operates with stoichiometric JP10-air at standard conditions and has a design thrust of 100 N. The fixed design thrust implies a relationship between the geometrical parameters of the engine and the cycle frequency. The tube design parameters, which are the diameter d, the length L, and the cycle frequency f, are subject to constraints. These are a maximum frequency limit, which is a function of the average filling velocity, and minimum dimensions proportional to the cell width ($d>\lambda/\pi$ for propagating detonations and $L>10\lambda$ for successful indirect detonation initiation). These relationships are summarized in a design surface in the (f, d, L) parameter space, given in Figure 31. Several additional issues were identified in addition to these calculations, including frequency limits due to filling and mixing, mixture sensitivity, efficient detonation initiation, liquid fuel injection system, multi-cycle operation, drag and flow losses, and engine operational envelope.
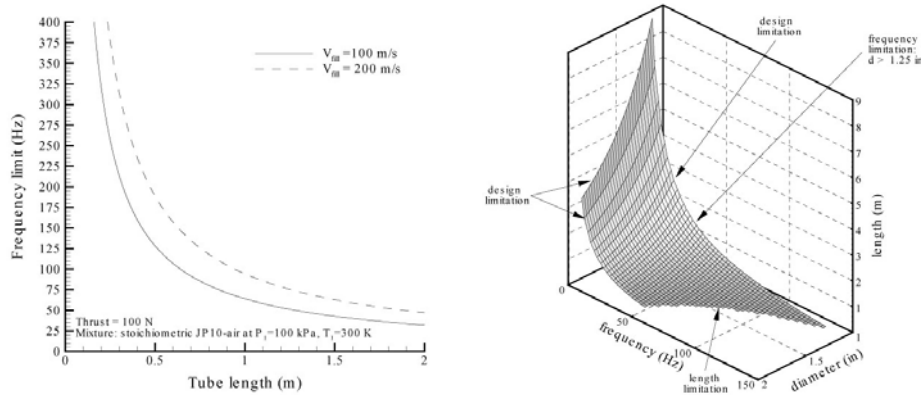

Figure 31. Estimate of PDE frequency limits and PDE design surface.

The structural aspects include engine geometry, mass, yield stress, structural resonance due to flexural wave excitation, critical flaw size, and fracture toughness. The yield stress criterion was used to determine the minimum wall thickness of an unflawed tube for four materials: aluminum, inconel, steel, and silicone nitride. Structural resonance due to flexural wave excitation was taken into account in these calculations. Fracture mechanics was used to predict critical flaw sizes for a detonation tube. The engine thrust-to-weight ratio was estimated based on the yield stress criterion for various tube lengths and diameters. Additional structural issues were highlighted such as impulsive thermomechanical fatigue, fracture due to single-cycle detonation loading, and plastic creep due to cyclic detonation loading.
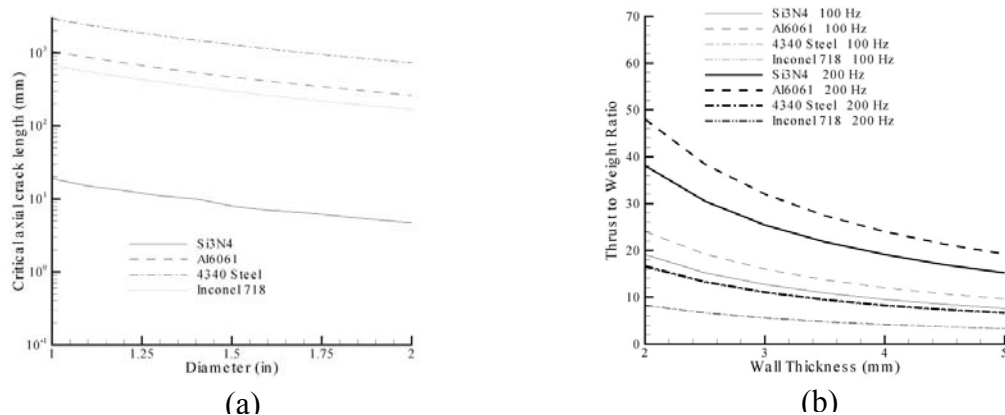
(a)   (b)

Figure 32. a) Critical flaw size versus tube diameter (fixed 2-mm wall thickness) and b) thrust-to-weight ratio versus wall thickness (fixed 1.5-in tube diameter).

Summary

Caltech has investigated fundamental detonation physics, detonation initiation techniques, fuel physical properties, detonation cell widths, impulse measurements and modeling for detonation tubes, and the structural aspects of detonation tubes.   Significant accomplishments include:

1. Visualization of detonation structure using PLIF in propagating detonations. Observations of "keystones" and correlation of keystones to transverse wave structure.
2. Measurement of detonation diffraction and development of a simple model for correlating critical diffraction diameter to chemical kinetic and gasdyamic properties of propagating detonations.
3. Measurement of detonation cell widths in mixtures of JP10 and air over a range of equivalence ratios, initial pressure, addition of small HC fuels.
4. Development of detonation initiation technique based on torodial imploding waves.
5. Direct measurement of detonation tube impulse for hydrocarbon fuels using the ballistic pendulum technique.
6. Development of an analytical model for impulse from a detonation tube and validation against single-cycle and multi-cycle experiments.
7. Measurement and analysis of structural response of tubes to detonation loading, including elastic response, plastic response, and fracture thresholds.
8. Design parameter studies examining the trade-off between structural, geometrical, and combustion parameters.

The results of these studies have been documented in over 15 conference proceedings, journal publications, and Caltech technical reports. We have presented our work at international and national meetings on combustion and propulsion. The results are available on-line from the Explosion Dynamics Web page in the form of electronic documents, databases, and spreadsheets. Over eight graduate students have participated in the program, five MS projects have been performed, one PhD has been completed, and four more are in progress on topics related to PDE science and technology.

Bibliography

[1] Schultz, E., Wintenberger, E., Shepherd, J.E., "Investigation of deflagration-to-detonation transition for application to pulse detonation engine ignition systems", in Proceedings of the 16th JANNAF Propulsion Symposium, Chemical Propulsion Information Agency, 1999.

[2] Lieberman, D.H., Parkin, K., and Shepherd, J.E., "Detonation Initiation by a Hot Turbulent Jet for use in Pulse Detonation Engines" AIAA 02-3909, 38th AIAA/ASME/SAE/ASEE Joint Propulsion Conference and Exhibit, July 7-10 2002, Indianapolis, IN

[3] Quirk, J.J., "Amrita: A computational facility (for CFD modeling)". In 29th Computational Fluid Dynamics Lecture Series, Von Karman Institute, 1998

[4] Izumi, K., Aso, S., Nishida, M., "Experimental and computational studies of focusing processes in shock waves reflected from parabolic reflectors," Shock Waves 3, 341-345, 1994.

[5] Bartenev, A.M., Khomik, B.E., Gelfand, B.E., Gronig, H., Olivier, H., "Effect of reflection type on detonation initiation at shock wave focusing," Shock Waves 10, 197-204, 2000.

[6] Manzhalei V.I., "Detonation Regimes of Gases in Capillaries", Fiz. Goren. Vzryva, 28, 3, p93-99, 1992

[7] Jackson, S.I., and Shepherd, J.E., "Initiation Systems for Pulse Detonation Engines" AIAA 02-3627, 38th AIAA/ASME/SAE/ASEE Joint Propulsion Conference and Exhibit, July 7-10 2002, Indianapolis, IN

[8] Austin, J.M., and Shepherd, J.E., "Detonations in Hydrocarbon Fuel Blends", accepted Combust. Flame, 2002

[9] Brabbs, T.A. and Merritt, S.A. "Fuel-rich Catalytic Combustion of a High Density Fuel" Technical report 3281, NASA, 1993

[10] Tieszen, S.R., Stamps, D.W., Westbrook, C.K., Pitz, W.J., "Gaseous Hydrocarbon-Air Detonations", Combust. Flame, 84 (3):376-390, 1991

[11] White, D., "Turbulent Structure in Gaseous Detonations" Phys. Fluids 4, 465-480, 1961

[12] Voitsekhovskii, B., Mitrofanov, V., and Topchian, M., "Struktura Fronta Detonastii i Gaza" Akad. Nauk. SSSR, Novosibirsk, Translation: The structure of a detonation front in gases, Rep. FTD-MT-64-527, Foreign Technology Division, Wright-Patterson A.F.B., Ohio, 1966

[13] Edwards, D., Hooper, G., and Meddins, R., "Instabilities in the Reaction Zones of Detonation Waves" Astronaut. Acta, 17 (4-5), 475-485, 1972

[14] Takai R., Yoneda,K., and Hikita, T., "Study of Detonation Wave Structure" 15th Int. Symp. Combust. p69-78, 1974

[15]Pintgen, F., Eckett, C., Austin, J.M., Shepherd, J.E, "Direct Observations of Reaction Zone Structure in Propagating Detonations", accepted Combust. Flame, 2002. see also AIAA 02-0773

[16]Pintgen, F., Austin, J.M., and Shepherd, J.E, "Detonation Front Structure: Variety and Characterization" Int. Colloquium on Advances in Confined Detonations, July 2-5 2002, Moscow

[17] Schultz, E., "Detonation Diffraction through an Abrupt Area Expansion", PhD thesis, California Institute of Technology, 2000

[18] Cooper, M., Jackson, S., Austin, J.M., Wintenberger, E., and Shepherd, J.E., "Direct Experimental Impulse Measurements for Detonations and Deflagrations", accepted J. Prop. Power 2002, see also AIAA 01-3812

[19] M. Kaneshige and J.E. Shepherd. "Detonation database" Technical Report FM97-8, GALCIT, July 1997. See also the electronic hypertext version at http://www.galcit.caltech.edu/detn_db/html/.

[20] Li, C., Kailasanath, K., and G. Patnaik, "A Numerical Study of Flow Field Evolution in a Pulsed Detonation Engine", 38th AIAA Aerospace Sciences Meeting and Exhibit, Jan 10-13, 2000, Reno, NV, AIAA02-0314

[21]Zhdan, S. A., Mitrofanov, V. V., and Sychev, A. I., "Reactive Impulse from the Explosion of a Gas Mixture in a Semi-Infinite Space," Combustion, Explosion and Shock Waves, Vol. 30, No. 5, 1994, pp. 657-663

[22] Kennedy, J. E., "The Gurney Model of Explosive Output for Driving Metal," Explosive Effects and Applications, edited by J. A. Zuker and W. P. Walters, chap. 7, Springer, New York, 1998, pp. 221-257.

[23] Cooper, M., and Shepherd, J.E., "The Effect of Nozzles and Extensions on Detonation Tube Performance" AIAA 02-3628, 38th AIAA/ASME/SAE/ASEE Joint Propulsion Conference and Exhibit, July 7-10 2002, Indianapolis, IN

[24] Wintenberger, E., Austin, J.M., Cooper, M., Jackson, S., and Shepherd, J.E., "An Analytical Model for the Impulse of a Single-Cycle Pulse Detonation Tube" accepted J. Prop. Power, 2002, see also AIAA 01-3811

[25] Schauer, F., Stutrud, J, Bradley, R., "Detonation initiation studies and performance results for pulsed detonation engines", AIAA 2001-1129

[26] Beltman, W. and J. Shepherd, "Linear elastic response of tubes to internal detonation loading," Journal of Sound and Vibration 252(4):617-655, 2002..

[27] Beltman, W., E. Burscu, J. Shepherd, and L. Zuhal, "The structural response of tubes to internal shock loading," Journal of Pressure Vessel Technology 121, 315-322, 1999.

[28] Lew, A. and M. Koslowski, "Plastic response of thin tubes to gaseous detonation waves," Ae104 Project Report, Graduate Aeronautical Laboratories, California Institute of Technology, 1999.

[29] Chao, T. and J. E. Shepherd, "Fracture response of externally flawed cylindrical shells to internal gaseous detonation loading," to appear in Proceedings of ASME Pressure Vessels and Piping Conference, Vancouver, British Columbia, Canada, August 4-8, 2002

[30] T. Chao, E. Wintenberger, and J. E. Shepherd, "On the Design of Pulse Detonation Engines" Explosion Dynamics Laboratory Report FM00-7, California Institute of Technology, January 2001

[31] Shepherd, J.E., Nuyt, C.D., Lee., J.J., "Flash Point and Chemical Composition of Aviation Kerosene (Jet A)". Explosion Dynamics Laboratory Report FM99-4, California Institute of Technology, December 1999